J. Chem. Thermodynamics 62 (2013) 211–221

Contents lists available at SciVerse ScienceDirect

J. Chem. Thermodynamics

journal homepage: www.elsevier.com/locate/jct

Standard Gibbs energies of formation and equilibrium constants from *ab-initio* calculations: Covalent dimerization of NO_2 and synthesis of NH_3

Neha Awasthi [a,*], Thomas Ritschel [b], Reinhard Lipowsky [a], Volker Knecht [a]

[a] Department of Theory & Biosystems, Max Planck Institute of Colloids and Interfaces, Am Mühlenberg 1, D-14476 Potsdam, Germany
[b] Institut für Chemie, Universität Potsdam, Karl-Liebknecht-Str. 24–25, D-14476 Potsdam, Germany

ARTICLE INFO

Article history:
Received 4 January 2013
Received in revised form 11 March 2013
Accepted 15 March 2013
Available online 30 March 2013

Keywords:
Equilibrium constants
Thermochemical properties
Ab-initio calculations

ABSTRACT

Standard quantum chemical methods are used for accurate calculation of thermochemical properties such as enthalpies of formation, entropies and Gibbs energies of formation. Equilibrium reactions are widely investigated and experimental measurements often lead to a range of reaction Gibbs energies and equilibrium constants. It is useful to calculate these equilibrium properties from quantum chemical methods in order to address the experimental differences. Furthermore, most standard calculation methods differ in accuracy and feasibility of the system size. Hence, a systematic comparison of equilibrium properties calculated with different numerical algorithms would provide a useful reference. We select two well-known gas phase equilibrium reactions with small molecules: covalent dimer formation of NO_2 ($2NO_2 \rightleftharpoons N_2O_4$) and the synthesis of NH_3 ($N_2 + 3\,H_2 \rightleftharpoons 2NH_3$). We test four quantum chemical methods denoted by G3B3, CBS-APNO, W1 and CCSD(T) with aug-cc-pVXZ basis sets (X = 2, 3, and 4), to obtain thermochemical data for NO_2, N_2O_4, and NH_3. The calculated standard formation Gibbs energies $\Delta_f G^\circ$ are used to calculate standard reaction Gibbs energies $\Delta_r G^\circ$ and standard equilibrium constants K^{eq} for the two reactions. Standard formation enthalpies $\Delta_f H^\circ$ are calculated in a more reliable way using high-level methods such as W1 and CCSD(T). Standard entropies S° for the molecules are calculated well within the range of experiments for all methods, however, the values of standard formation Gibbs energies $\Delta_f G^\circ$ show some dependence on the choice of the method. High-level methods perform better for the calculation of molecular energies, however, simpler methods such as G3B3 and CBS-APNO perform quite well in the calculation of total reaction energies and equilibrium constants, provided that the chemical species involved do not exhibit molecular geometries that are difficult to handle by the applied method. The temperature dependence of standard reaction Gibbs energy $\Delta_r G^\circ$ for the NH_3 reaction is discussed by using the calculated standard formation Gibbs energies $\Delta_f G^\circ$ of the reaction species at 298.15 K. The corresponding equilibrium constant K^{eq} as a function of temperature is found to be close to experimental values.

1. Introduction

Thermodynamics of equilibrium reactions provides valuable information about the underlying reaction mechanism. Accurate experimental measurements to determine equilibrium properties such as enthalpy, Gibbs energy of reaction and equilibrium constant, K^{eq}, are often challenging. Computational methods provide a useful tool to corroborate these experimental measurements. Molecular dynamics (MD) simulations have been used to predict K^{eq} for weak complexes with non-covalent interactions and the lifetime of non-covalently formed dimers [1]. Although MD simulations are useful for large systems and can include solvent interactions, the prediction of K^{eq} is limited in accuracy because of the classical treatment of formation and dissociation of reaction species. Quantum chemical calculations are useful to get accurate thermodynamic data [2] as well as information about dynamical properties such as reaction intermediates, activation energies, and rate constants [3].

Experimentally, the equilibrium constant K^{eq} can be determined by measurements of infrared (IR) or ultra-violet(UV)-visible spectra [4,5], or by measurements of the sound velocity in the equilibrium mixture [4]. For gas phase reactions, K^{eq} is also calculated from pressure measurements [4]. Equilibrium reactions are strongly temperature dependent [5] and direct experimental measurements can be conducted for a range of temperatures using methods such as flash photolysis-shock tube techniques [6]. The temperature dependence of K^{eq} is often used to calculate enthalpies and Gibbs energies of reactions [7,8]. Standard formation enthalpies, $\Delta_f H^\circ$, for molecules are determined from calorimetric experiments [9,10] or vapor pressure measurements [10]. K^{eq} for

* Corresponding author. Tel.: +49 331 567 9601.
E-mail address: neha.awasthi@mpikg.mpg.de (N. Awasthi).

0021-9614/$ - see front matter © 2013 Elsevier Ltd. All rights reserved.
http://dx.doi.org/10.1016/j.jct.2013.03.011

a reaction can also be calculated by constructing a reaction scheme [5], with Gibbs energies, $\Delta_r G$, and K^{eq} of intermediate reactions involved as input. Input values may be from sources that differ in accuracy (literature or additional experiments), which can give rise to possible discrepancies. K^{eq} values are extrapolated using thermodynamic data, which also contributes to the uncertainty. Many recent experimental calorimetry studies also include quantum chemical calculations to support experimental measurements [10–12]. Furthermore, unconventional reaction conditions (temperature, pressure, absence of catalysts, solvents) which are not easily accessible in a laboratory can be probed using simulations. In fact, density functional and other model chemistry simulation methods have been used to check experimental data, such as $\Delta_f H^\circ$, and to resolve discrepancies between reported values [13,14,11,15]. Ruscic *et al.* [16] presents a critical evaluation of thermochemistry data from various experimental sources (kinetic, spectroscopic, and ion cycle studies) for some organic radicals, and includes high-level theoretical calculations to settle discrepancies. Quantum chemical calculations have also been used to provide accurate structural parameters, such as the equilibrium N–H bond length in molecules including NH_3, using three different methods [17]. Demaison *et al.* [17] also provides the evolution of the estimates of the structure of NH_3 with time. Apart from stable molecules, thermochemical calculations are quite useful in the characterization of structural and thermochemical properties of radicals and ions, such as NH_4^+ [17] and $^{\cdot}NO_3$ [18].

For simple chemical reactions involving small molecules, quantum mechanical methods are efficient for calculating $\Delta_f H$, $\Delta_f G$, and $\Delta_r G$, and hence, predicting K^{eq}. Benchmark thermochemistry calculations have been reported in the literature for several molecular species and the NIST thermochemistry database is a collection of such data [19]. We emphasize that our investigation with the choice of reaction species using four different compound thermochemistry methods does not correspond to an existing entry in the database. In fact, our work reporting structural, vibrational and thermochemical data makes a useful addition to the NIST repository [19].

We consider two well investigated gas phase reactions involving small molecules consisting of less than 10 atoms, Covalent dimer formation of NO_2 and uncatalyzed synthesis of NH_3. Experimental values for K^{eq} are available for both of these reactions [4,20,21]. For the NO_2 reaction, a critical review of the measurements of K^{eq} as a function of temperature using several experimental techniques is provided in Ref. [4]. We note that the equilibrium constants for both these reactions have not been discussed from a computational perspective with comparison between several methods. We present a systematic study comparing four *ab-initio* methods such as G3B3, CBS-APNO, W1 and CCSD(T), of different accuracy and computational intensity, to calculate the Gibbs energies $\Delta_f G^\circ$, and $\Delta_r G^\circ$, as well as the equilibrium constants K^{eq}. To our knowledge, our study is the first comparing equilibrium constants obtained from different methods, and discussing the temperature dependence of calculated versus experimental equilibrium constants.

The four methods that we consider have been developed starting from different theoretical frameworks. Hence, there is a significant difference in their performance, with respect to accuracy and computational expense. However, the choice of a given method cannot be naively made on the basis of performance alone. The application of a particular method for a given molecule may lead to unexpected results, as we see later in our work. Therefore, it is useful to have studies that offer a comparative perspective and report interesting outliers/limitations for a method. Our work also contributes towards this goal. We use Ref. [22] as a source for experimental data, and we have checked that there are no computational results reported for the combination of reactions and methods that we study here.

The higher level methods, such as W1 and CCSD(T), though accurate, are not feasible for molecules that contain more than 10 atoms. Our study provides a comparison between different methods which can be used for a range of molecular sizes. We note that our aim is not to repeat the earlier works, which computed geometries and energies up to very high levels of accuracies (see Ref. [23]), but to show that one can study formation and equilibrium processes at an intermediate level of accuracy, with some extrapolation of the incompleteness of the basis set. Such computationally inexpensive methods are useful if one can expect to find reasonable agreement between calculated and experimental thermochemistry data. We compare our results, such as structural parameters, vibrational frequencies, and energies, with those of previous studies. There has been a previous quantum chemical calculation for the formation of oxides of nitrogen (NO_2 and N_2O_4 among others) [24] using the CCSD(T) method which reports structural parameters, enthalpies, entropy [24]. We show that our CCSD(T) data are consistent with the results in Ref. [24]. Our paper is organized as follows: Section 2 describes the details of the methods used. The results and the discussion are presented in Section 3, followed by conclusions in Section 4.

2. Method

We study two gas phase equilibrium reactions, covalent dimer formation of NO_2 and synthesis of NH_3, for which the experimental equilibrium data are given in table 1. The Gibbs energy $\Delta_r G$ for these equilibrium reactions can be expressed as

$$\Delta_r G = \Delta_r G^\circ + RT \ln Q, \tag{1}$$

where R is the gas constant and T the absolute temperature. Q is the reaction quotient, which is given by

$$Q \equiv \frac{(P_{N2O4}/P^\circ)}{(P_{NO2}/P^\circ)^2}, \tag{2}$$

for the NO_2 dimerization reaction, where P° is the standard pressure and P_{N2O4} or P_{NO2} denote the partial pressures for the product or reactant, respectively. At chemical equilibrium, $\Delta_r G = 0$ and Q becomes equal to the equilibrium constant K^{eq}, such that

$$\Delta_r G^\circ = -RT \ln K^{eq}. \tag{3}$$

The standard reaction Gibbs energy, $\Delta_r G^\circ$, is equal to the difference in the standard Gibbs energies of formation, $\Delta_f G^\circ$ [25], of the products and reactants. Hence, the equilibrium constant K^{eq} for the NO_2 reaction is given as

$$K^{eq} = e^{-\frac{1}{RT}(\Delta_f G^\circ_{N_2O_4} - 2\Delta_f G^\circ_{NO_2})}. \tag{4}$$

For the NH_3 reaction, as given in table 1, one has

$$K^{eq} = e^{-\frac{1}{RT}(2\Delta_f G^\circ_{NH_3} - \Delta_f G^\circ_{N_2} - 3\Delta_f G^\circ_{H_2})}. \tag{5}$$

The Gibbs energy of formation, $\Delta_f G^\circ_X$, is defined as the standard reaction Gibbs energy for the formation of the compound from its

TABLE 1
Equilibrium reactions of covalent dimer formation from NO_2 and synthesis of NH_3. Equilibrium constants and reaction Gibbs energies correspond to $T = 298.15$ K and 1 atm pressure. Data for the NO_2 reaction were obtained from experiments [4], previous quantum-chemical calculations [24], and thermochemical tables [20]. Data for the NH_3 reaction were obtained from [20].

Reaction	K^{eq}	$\Delta_r G$/kJ · mol^{-1}
$2NO_2 \rightleftharpoons N_2O_4$	6.54–10.64	−4.73 to −5.86
$N_2 + 3H_2 \rightleftharpoons 2NH_3$	5.94×10^5	-32.90

elements in their reference states, where reference state is the most stable state of the element at the specified temperature (298.15 K for our calculations) and pressure of 1 bar [25].

The equilibrium constant calculated via $\Delta_r G^\circ$ using statistical thermodynamic calculations is dimensionless. According to the IUPAC recommendation [26], the dimensionless equilibrium constant defined at standard conditions is also called the thermodynamic equilibrium constant. However, experimental studies often report equilibrium constants in units of pressure for gas phase reactions, which will be denoted as K_p. For the reactions shown in table 1, the equilibrium constants K_p are defined in terms of the partial pressures at equilibrium and given by

$$K_p = \frac{(P_{N2O4})}{(P_{NO2})^2} \tag{6}$$

and

$$K_p = \frac{(P_{NH3})^2}{(P_{N2})(P_{H2})^3}. \tag{7}$$

Using the ideal gas law for a reaction in the gas phase at constant temperature (standard temperature 298.15 K in our case), we obtain the relation

$$K_p = K^{eq}(P^\circ)^{\Delta n}, \tag{8}$$

where P° is the standard pressure, 10^5 Pa or 1 bar and Δn denotes the difference between the sum of the stoichiometries of the products and the reactants. For the NO_2 dimerization reaction, $\Delta n = -1$ while for the synthesis of NH_3, $\Delta n = -2$ (see table 1). We use the dimensionless standard equilibrium constant, denoted by K^{eq} in our work, and all experimental values of K_p are duly converted for consistent comparison.

The standard formation Gibbs energy, $\Delta_f G^\circ_X$, was determined via *ab-initio* calculations using the Gaussian 03 [27] and MOLPRO [28] packages. Geometry optimizations and thermochemistry calculations were performed using the G3B3 [29], CBS-APNO [30], W1 [31], and CCSD(T) [32] methods for the NO_2, N_2O_4 and NH_3 molecules in the gas phase. In order to calculate formation energies, we also performed the same set of calculations for the N_2, O_2, and H_2 molecules.

These standard methods differ in the underlying theoretical procedure as well as the accuracy. G3B3, CBS-APNO, and W1 are compound thermochemistry methods, which employ several steps of calculations using various basis sets and correction factors (except W1). Hence, there is a dependence of calculated Gibbs energies and equilibrium constants on the basis sets and the level of theory. G3B3, one of the Gaussian model chemistry (GX) methods [33], uses the B3LYP functional for structure and frequency (at the B3LYP/6-31 G(d) level) calculations. Calculations do not require excessive time or computing resources, and thermochemistry data are obtained within the accuracy of $\simeq \pm 4.13$ kJ · mol^{-1} [29].[1] The CBS-APNO method utilizes the asymptotic convergence of pair natural orbitals to overcome the error introduced due to the single-electron basis set truncation [30]. This method includes higher order correlations, as compared to GX methods, with a relatively smaller basis set. The calculated energy is extrapolated to the complete basis limit, which improved the accuracy to $\simeq \pm 2.09$ kJ · mol^{-1} [30].[2] at a relatively low computational expense. Frequencies are calculated at the HF/6-311 G(d,p) level [30]. Both GX and CBS methods have issues with spin-contamination in open-shell molecules, low-lying virtual orbitals and molecules having multiple lone pairs on the same atom.

The W1 level of theory [31] performs a CCSD calculation [32] using Dunning's augmented polarized correlation-consistent polarized valence basis sets (aug-cc-pVXZ avdz) [34,35] and uses no empirical corrections like the GX and CBS methods. It is one of the most intensive methods with an accuracy on the order of $\simeq \pm 1.25$ kJ · mol^{-1} [31].[3] The computational cost makes it feasible for small molecules only. For the open-shell systems NO_2 and O_2, the spin-unrestricted W1U method is used. Frequency calculation is done at the B3LYP/aug-cc-pVTZ level. We also performed coupled cluster calculations with single and double excitation and non-iterative triples [32] CCSD(T) (for closed shell systems) and UCCSD(T) using aug-cc-pVXZ avdz basis sets at the X = 2, 3, 4 (=D, T, Q for double-ζ, triple-ζ, and quadruple-ζ, respectively) levels, closely following the procedure described in [24]. This approach starts with geometry optimization and computation of vibrational frequencies using the aug-cc-pVDZ basis set. For open shell molecules, like NO_2 and O_2, spin-unrestricted UCCSD(T) calculations (based on ROHF orbitals) are conducted. In order to estimate the electronic energies in the complete basis set (CBS) limit, single point calculations are performed for the triple-ζ and quadruple-ζ basis sets (aug-cc-pVTZ and aug-cc-pVQZ, respectively), using the geometries obtained at the double-ζ level. Following the work of Peterson *et al.* [36], the CBS-extrapolated energies (E_{cbs}) are obtained by representing the calculated energies as the following mixed exponential plus Gaussian function:

$$E[X] = E_{cbs} + ae^{-(X-1)} + be^{-(X-1)^2}. \tag{9}$$

Here, X denotes the ordinal number for the basis set as explained above, E_{cbs} is the extrapolated energy in the complete basis set limit, whereas a and b are fitting parameters. The expected accuracy of this method is $\simeq \pm 2.0$ kJ · mol^{-1} [37].

In order to determine $\Delta_f G^\circ_X$ for a compound X of composition A_mB_n, thermochemistry calculations using a particular method are performed for A_mB_n, and the stable form of constituent elements A and B. Effectively, one considers the formation of the molecule from its constituent elements, being diatomic gases H_2, N_2, and O_2 in our case.

We directly compute of the enthalpies and Gibbs energies by taking the appropriate differences in energies according to the formation reactions. This can be done since all the reference elemental standard states are diatomic gases (H_2, N_2, and O_2). Furthermore, this procedure does not require the actual computation of atomization energies which might be problematical for O and N, e.g., due to spin contributions. It should be noted that this is in contrast to the procedure based on atomization energies [38,39] which is typically used for molecules containing carbon or other elements, for which the computation of the elemental standard states is not feasible. This latter procedure does not correspond to a full *ab-initio* calculation since it also makes use of experimental data. In contrast, we use an unbiased *ab-initio* approach. We note that formation energies can also be calculated accurately using isodesmic reactions. However, in our case of simple gas phase reaction with few species, the calculation of formation energies using formation reactions is quite accurate and reasonable.

It is required that the enthalpies and Gibbs energies are calculated for optimized structures corresponding to a local minima. To validate this, vibrational frequencies were calculated for each species, and compared with available experimental data [20]. Unless stated otherwise, all calculations were performed at

[1] Error is the average absolute deviation from experiment in energies calculated for a test set with 299 molecules.

[2] Error is the mean absolute deviation of a model from experiment, for the 125 energies of the G2 test set. The maximum deviation from experiment observed within the test set is 6.27 kJ · mol^{-1}.

[3] Error is the mean absolute error and the method includes only a single, molecule-independent empirical parameter.

298.15 K and 1 atm pressure. The frozen core approximation was used for all calculations. We note that standard pressure is 1 bar for the definition of $\Delta_f G^\circ_X$, however, in both MOLPRO and Gaussian, thermochemical calculations assume a pressure of 1 atm (=1.01325 bar). Hence, one expects a deviation of $\simeq$1% between calculated and experimental data.

3. Results

The results in this section are organized as follows. We first summarize the structural parameters such as bond lengths, bond angles and vibrational frequencies. Thermochemistry data such as $\Delta_f H^\circ$, S°, and $\Delta_f G^\circ$ are given in Section 3.2, followed by equilibrium constants. Finally, in Section 3.4, the temperature dependence of $\Delta_f G^\circ$ is discussed.

3.1. Structural parameters and vibrational frequencies

Structural data for the reaction species involved in the two equilibrium reactions described in Section 2 are shown in table 2. Experimental data are taken from [40] for N_2O_4, and from [41] for NO_2 and NH_3. The structural data we report for the three molecules are a set for comparison between the four methods (see Section 2 for details) tested in this work. Some of the methods we test have been reported for one of the species earlier [24,23,42]. We present all our results for the sake of completeness.

Table 2 shows the comparison of bond lengths and bond angles for the equilibrated structures of N_2, H_2, O_2, NH_3, NO_2 and N_2O_4 calculated for all the four methods considered. In fact, we observe that structural parameters for small molecules can be reproduced with little computational cost and time, using methods such as G3B3. We see a consistent agreement between calculated and experimental parameters for all the three molecules, for the four methods we have tested.The bond lengths for N_2, H_2 and O_2 calculated in our study are in good agreement with those predicted from experiments [22]. The bond lengths obtained at the CCSD(T)/aug-cc-pVDZ level are typically a bit too large, especially for the diatomics, which is due to the relatively small basis set.

For NH_3, a dummy atom denoted as X was placed on the C_3 axis above the N atom in NH_3 in order to obtain the optimized structure with the correct C_{3v} symmetry. The improper dihedral angle of 120 degrees was kept constant for the geometry optimization. Bond lengths and angles calculated using the W1 method are in best agreement with the experimental data, while the CBS-APNO parameters show the largest deviation from the experimental numbers, with a smaller length for the N–H bond and a larger H–N–H bond angle. Our calculations for NH_3 using the CCSD(T)/aug-cc-pVDZ method reproduce the data reported by Lin *et al.* [23,17]. For NO_2, both W1 and CCSD(T) give values close to experiments. For N_2O_4, the results from W1 agree well with experiments and we observe that data from G3B3 are also in good agreement with experimental values. The structure of N_2O_4 is planar (D_{2h} symmetry) and the dihedrals angles (O–N–N–O) are 0 and 180 degrees. The parameters for NO_2 and N_2O_4 calculated in this work using the CCSD(T) method agree well with those reported in an earlier study [24]. For CBS-APNO, we note a rather short N–N bond (0.1688 nm) in the N_2O_4 molecule. This indicates that the underlying RHF level of theory used in CBS-APNO for obtaining the geometry partly fails here. Our CBS-APNO N–O and N–N bond lengths for N_2O_4 are identical to those reported in [42].

Table 4 shows unscaled vibrational frequencies for NH_3, NO_2 and N_2O_4. We compare the data obtained from the four different methods and also with experiments. Experimental frequencies for N_2O_4 are taken from [43], for NO_2 from [44,45] and for NH_3 from [44]. All frequencies, for the three reaction species, calculated using W1 and CCSD are in better agreement with experiments as compared to those calculated using the G3B3 and CBS methods. For NH_3, the maximum deviation from the experimental measurement is observed for the a_1 mode of 950 cm^{-1}, for all the four methods. This mode corresponds to the umbrella mode with symmetric deformation motion. The other modes agree with the experimental data, with W1 and CCSD(T) performing better, as expected. We see a maximum deviation for the CBS-APNO frequencies, and this can be attributed to the rather strained optimized structure of NH_3 modeled by this method.

For NO_2 and N_2O_4, the vibrational frequencies calculated using CCSD(T) are consistent with those reported in [24] and in best agreement with experiments. Those calculated using W1 are also in good agreement with experiments. Among the four methods, the CBS-APNO frequencies show the largest deviation for both NO_2 and N_2O_4, for all the modes. In case of N_2O_4 the largest deviations are apparent for the symmetric stretch mode a_g which is directly affected by the short N–N distance. For the other modes, the effect is less pronounced.

Vibrational frequencies are obtained in the harmonic approximation. Scaling factors, between 0.8–1.0, are defined by the average ratio of experimental to calculated frequencies. These factors compensate for the approximation used in the calculations and the inaccuracies of a given level of theory. Table 3 shows the scaling factors calculated from our data, averaged over all modes for each molecule, for a given method. Values in parentheses are scaling factors recommended for a particular method from other studies [29–31]. We observe that the scaling factor for G3B3 is

TABLE 2
Comparison of optimized structural parameters for species involved in equilibrium reactions calculated with the quantum-chemical G3B3, CBS-APNO, W1, and CCSD(T) methods. Bond distances (r) are given in nm and bond angles (a) in degrees. X denotes a dummy atom lying on the C_3 axis above the N atom in NH_3. The improper dihedral angle (120 degrees) was kept constant during geometry optimization. The N_2O_4 molecule has a planar geometry and the dihedral angles are exactly 0 and 180 degrees. Experimental parameter values were obtained from [22] for diatomic molecules, from [41] for NH_3 and NO_2, and from [40] for N_2O_4.

Molecule (symmetry)	Parameter	G3B3	CBS-APNO	W1	CCSD(T)	Experiment
N_2 ($D_{\infty h}$)	$r_{N\text{-}N}$/nm	0.11055	0.11041	0.10915	0.1121	0.1098
H_2 ($D_{\infty h}$)	$r_{H\text{-}H}$/nm	0.07428	0.07355	0.07409	0.0762	0.0741
O_2 ($D_{\infty h}$)	$r_{O\text{-}O}$/nm	0.12146	0.11569	0.12059	0.1220	0.1208
NH_3 (C_{3v})	$r_{N\text{-}H}$/nm	0.1019	0.1000	0.1014	0.1024	0.1012
	$a_{H\text{-}N\text{-}H}$	105.785	107.46	106.50	105.9	106.67
	$a_{X\text{-}N\text{-}H}$	111.94	115.40	113.36	112.8	112.15
NO_2 (C_{2v})	$r_{N\text{-}O}$/nm	0.1203	0.1194	0.1192	0.1211	0.1193
	$a_{O\text{-}N\text{-}O}$	133.85	134.43	134.40	133.9	134.1
N_2O_4(D_{2h})	$r_{N\text{-}N}$/nm	0.1782	0.1688	0.1751	0.1780	0.1782
	$r_{N\text{-}O}$/nm	0.1196	0.1190	0.1194	0.1204	0.1190
	$a_{N\text{-}N\text{-}O}$	112.65	112.85	112.58	112.6	112.3
	$a_{O\text{-}N\text{-}O}$	134.69	134.29	134.83	134.80	135.4

TABLE 3
Scaling factors for vibrational modes, which represent the average ratio of experimental to calculated vibrational frequencies, as calculated with the G3B3, CBS-APNO, W1, and CCSD(T) methods. For a given molecule, each factor is an average over all the modes. Values in parentheses indicate scaling factors as recommended in previous studies [29–31].

Molecule	G3B3 (0.96)	CBS-APNO (0.9251)	W1 (0.985)	CCSD(T) (None)
NH_3	0.93	0.88	0.95	0.95
NO_2	0.96	0.85	0.96	0.99
N_2O_4	0.96	0.81	0.97	1.00

TABLE 4
Comparison of vibrational modes for species involved in equilibrium reactions calculated with the quantum-chemical G3B3, CBS-APNO, W1, and CCSD(T) methods. Frequencies are unscaled and in units of cm^{-1}. Experimental frequencies are taken from [43–45].

Molecule (symmetry)	Mode symmetry (cm^{-1})	G3B3	CBS-APNO	W1	CCSD(T)	Experiment
NH_3 (C_{3v})	a_1	1129	1145	1063	1069	950
	a_1	3438	3687	3461	3433	3337
	e	1726	1802	1676	1650	1627
	e	3570	3809	3578	3570	3444
NO_2 (C_{2v})	a_1	748	851	766	743	750
	a_1	1404	1613	1392	1333	1318
	b_2	1720	1878	1697	1650	1618
N_2O_4(D_{2h})	a_g	299	463	299	273	282
	a_g	838	979	853	804	807
	a_g	1460	1613	1450	1389	1383
	a_u	95	71	88	86	82
	b_{1u}	756	902	765	737	755
	b_{1u}	1330	1531	1308	1273	1261
	b_{2g}	681	893	703	677	657
	b_{2u}	230	371	228	222	265
	b_{2u}	1856	2031	1826	1787	1757
	b_{3g}	500	648	500	462	480
	b_{3g}	1829	1999	1794	1740	1718
	b_{3u}	434	598	443	430	425

within the range recommended for NO_2 and N_2O_4 and a slightly lower value for NH_3. For CBS-APNO, the scaling factor we obtain is quite low as compared to the expected value of 0.9251. The CBS-APNO method is known to have issues with the geometries of nitrogen oxide species [42]. This drawback is highlighted further in the thermochemistry data and is discussed in detail in the following subsection. For W1, the scaling factor is recommended to be 0.985 for the fundamental modes and our data are close, though somewhat below this value. CCSD(T) frequencies are typically reported unscaled and no scaling factors are applied. It is important to note that we report unscaled frequencies for all the molecules from the four methods. These scaling factors are a measure for the agreement between experimental and computed frequencies, and therefore also an indirect measure for anharmonicity effects in such calculations.

The optimized structures for all the species reproduced the correct symmetry group for all the four methods, and no degree of freedom was missing in the vibrational analysis. In particular, the deviations between calculated and experimental frequencies of N_2O_4 cannot be attributed to lack of proper symmetry. For N_2O_4, we observe that there are five low lying modes (table 4) which need careful examination with respect to the harmonic oscillator approximation used for vibrational calculations. Our calculations, for all the four methods, detect the a_u mode (82 cm^{-1}, see table 4) as a hindered internal rotor, which corresponds to the rotation of the two NO_2 groups against each other. Hence, the electronic energy and entropy calculated using the harmonic oscillator approximation for N_2O_4 should be corrected by the contribution from this internal rotation mode.

TABLE 5
Electronic energy E, and entropy, S, corrected for the hindered rotor analysis performed for the a_u vibrational mode for N_2O_4. Subscripts *ho* and *hr* refer to contributions due to this mode obtained using the harmonic oscillator and hindered rotor, analysis respectively. Scaling factor and reduced moment used for the hindered rotor analysis are also provided. Scaled and unscaled refer to data obtained with and without the use of a method specific scaling factor for the vibrational frequency. The correction in E, $E_{corr} = E_{hr} - E_{ho}$, and likewise for S. Electronic energies are in $kJ \cdot mol^{-1}$ and entropies in $J \cdot K^{-1} \cdot mol^{-1}$.

Parameter	G3B3	CBS-APNO	W1	CCSD(T)
a_u Vibration/cm^{-1}	95	71	88	86
Scaling factor	0.96	0.9251	0.985	1.0
Reduced moment/amu × $bohr^2$	17.38	16.11	17.11	17.64
E_{ho} (unscaled)/$kJ \cdot mol^{-1}$	2.522	2.503	2.516	2.515
E_{hr} (unscaled)/$kJ \cdot mol^{-1}$	2.583	2.658	2.592	2.590
E_{corr} (unscaled)/$kJ \cdot mol^{-1}$	0.061	0.155	0.076	0.075
S_{ho} (unscaled)/$J \cdot K^{-1} \cdot mol^{-1}$	14.872	17.261	15.498	15.631
S_{hr} (unscaled)/$J \cdot K^{-1} \cdot mol^{-1}$	15.255	18.180	15.970	16.104
S_{corr} (unscaled)/$J \cdot K^{-1} \cdot mol^{-1}$	0.383	0.919	0.472	0.473
E_{ho} (scaled)/$kJ \cdot mol^{-1}$	2.519	2.500	2.515	
E_{hr} (scaled)/$kJ \cdot mol^{-1}$	2.586	2.691	2.594	
E_{corr} (scaled)/$kJ \cdot mol^{-1}$	0.067	0.191	0.079	
S_{ho} (scaled)/$J \cdot K^{-1} \cdot mol^{-1}$	15.205	17.902	15.622	
S_{hr} (scaled)/$J \cdot K^{-1} \cdot mol^{-1}$	15.629	19.035	16.113	
S_{corr} (scaled)/$J \cdot K^{-1} \cdot mol^{-1}$	0.424	1.133	0.491	

Table 5 shows the energetic and entropic contributions of the a_u mode calculated with the harmonic oscillator and the hindered rotor analysis at 298 K for all four methods. The difference between the two contributions is calculated using the Pitzer–Gwinn scheme [46,47]. Corrections were calculated using the respective a_u vibrational frequencies corresponding to each method. Corrections in electronic energy, E_{corr} are small (0.06–0.08 $kJ \cdot mol^{-1}$) for G3B3, W1 and CCSD(T), while the largest $E_{corr} \simeq 0.19\ kJ \cdot mol^{-1}$ for CBS-APNO. The corrections for W1 and CCSD(T) values are almost equal. This is expected since the frequencies are similar and the scaling factor for W1 is close to unity. There is no significant difference between the energy corrections for scaled and unscaled analysis, except for CBS-APNO. We recall that the deviation from experimental value for the CBS-APNO a_u mode is the largest amongst the four methods. Adding the hindered rotor correction does not improve the energies significantly, although the correction is relatively larger for the CBS-APNO value as compared to other methods. A similar trend is observed for the entropic correction S_{corr} between the four methods. However, the inclusion of the scaling factors has some impact on the entropy corrections, which are significantly larger than the unscaled ones. S_{corr} for CBS-APNO is more than twice as large as the other ones. This difference reflects the lower predicted frequency (71 vs. 86/88/95), lower scaling factor (0.9251 vs. 0.96/0.985) and the smaller reduced moment (primarily attributed to the shorter N–N distance).

Since compound methods use a scaling factor (e.g., 0.985 for W1) for the harmonic frequencies, the same factor should also be used for the hindered rotor correction. However, we found that *Gaussian* by default uses unscaled frequencies for the hindered rotor analysis performed for the compound methods. Therefore, the values given in table 5 are recomputed manually using the proper scaling factors following the Pitzer–Gwinn scheme [47] as used in *Gaussian*. In particular, this means that the procedure as done by *Gaussian* (using the unscaled frequencies) slightly overcompensates the errors caused by the improper vibration. For the CCSD(T) results, the same Pitzer–Gwinn scheme was used, since MOLPRO does not provide a hindered rotor detection and correction at all. For the MOLPRO computation a reduced moment of 17.64 amu ×

TABLE 6
Ground state electronic energy at 0 K, E_0, and zero point energy correction, *ZPE*, absolute enthalpy at 0 K, H_0, absolute enthalpy at 298 K, H_{298}, and absolute Gibbs energy at 298 K, G_{298} for species involved in the two equilibrium reactions calculated using the G3B3, CBS-APNO, W1, and CCSD(T) methods. For CCSD(T), E_0 denotes the extrapolated electronic energy for the complete basis set limit, E_{cbs}. All energies are in hartree.

Molecule	Parameter (hartree)	G3B3	CBS-APNO	W1	CCSD(T)
N_2	*ZPE*	0.005375	0.005775	0.005497	0.005281
	E_0	−109.493406	−109.533219	−109.585670	−109.420888
	H_{298}	−109.484727	−109.524140	−109.576868	−109.412302
	G_{298}	−109.506481	−109.545833	−109.598599	−109.434084
H_2	*ZPE*	0.009739	0.009683	0.009918	0.009896
	E_0	−1.177214	−1.174966	−1.174592	−1.174177
	H_{298}	−1.164170	−1.161978	−1.161369	−1.160976
	G_{298}	−1.178962	−1.176752	−1.176161	−1.175816
O_2	*ZPE*	0.003628	0.004216	0.003655	0.003567
	E_0	−150.256362	−150.315559	−150.414423	−150.199643
	H_{298}	−150.249426	−150.308037	−150.407461	−150.192768
	G_{298}	−150.272713	−150.331229	−150.430734	−150.216547
NH_3	*ZPE*	0.033164	0.033840	0.033740	0.034049
	E_0	−56.541457	−56.559731	−56.586362	−56.503766
	H_{298}	−56.504484	−56.522081	−56.548810	−56.465907
	G_{298}	−56.526335	−56.543883	−56.570650	−56.487773
NO_2	*ZPE*	0.008471	0.009153	0.008654	0.008490
	E_0	−204.992493	−205.073107	−205.194993	−204.89838
	H_{298}	−204.980128	−205.060088	−205.182459	−204.886007
	G_{298}	−205.007412	−205.087187	−205.209690	−204.913297
N_2O_4	*ZPE*	0.022557	0.025510	0.023025	0.022523
	E_0	−410.011588	−410.170385	−410.416690	−409.823535
	H_{298}	−409.982671	−410.139091	−410.387376	−409.794638
	G_{298}	−410.017103	−410.172529	−410.421717	−409.829147

bohr^2 was used. Thermochemical quantities reported in the following subsection include the hindered rotor correction for N_2O_4 at 298 K.

It is important to note that energies are obtained at the final step of the compound thermochemistry methods, however frequencies are calculated at intermediate levels. The CBS-APNO method uses a larger basis set at the HF level, as compared to G3B3 for calculation of frequencies, however, G3B3 performs better due to inclusion of correlation with the B3LYP functional. With the W1 method, using a correlation consistent basis set [34,35] along with the B3LYP functional, improves the results further, as seen in table 4.

Thermochemical data are obtained by combining the vibrational data with the electronic energies calculated with a given method. Table 6 shows the zero point energy correction, *ZPE*, and the electronic reference energy at 0 K, E_0, for all the reaction species. The *ZPE* are scaled by the respective scaling factor for a given method. E_0 is the reference energy to which the *ZPE* and the thermal corrections are added to obtain the thermochemical quantities for a given temperature. For standard methods (such as RHF and B3LYP) E_0 is the electronic energy. However, for the compound methods, the reference energy itself is the sum of the electronic energy plus some corrections. Hence, we denote E_0 as the electronic reference energy.

For CCSD(T) data, calculated electronic energies are extrapolated to the complete basis set limit (E_{cbs}). This extrapolation of CCSD(T) energies is described in Section 2. Fig. 1 shows the CBS-extrapolated energies obtained using the mixed exponential plus Gaussian function (equation (9)) for the CCSD(T) calculations performed for H_2, N_2, O_2, NO_2, NH_3, and N_2O_4. As expected, increasing the cardinal number of the basis set, we observe the electronic energy tending towards the (extrapolated) basis set limit. The CCSD(T) E_0 values listed in table 6 are E_{cbs} values.

Furthermore, the absolute enthalpy at 0 K, H_0, absolute enthalpy at 298 K, H_{298}, and absolute Gibbs energy at 298 K, G_{298} for all the species are presented in table 6. These are the quantities used for the calculation of the formation enthalpies and Gibbs energies in the following subsection.

3.2. Thermochemistry: enthalpy of formation, Gibbs energy of formation and absolute entropy

In this section the results for $\Delta_f H^\circ_X$, S_X, and $\Delta_f G^\circ_X$, for NH_3, NO_2 and N_2O_4 in the gas phase at standard conditions (298.15 K and 1 atm) are presented. The respective formations of NH_3, NO_2 and N_2O_4 are considered from N_2, H_2, and O_2 in appropriate stoichiometric ratio. $\Delta_f H^\circ_X$ and $\Delta_f G^\circ_X$ for H_2, N_2, O_2 corresponding to the stable forms of the respective elements are set to zero.[4] Absolute entropies S_X for all species are reported from the respective calculations of NH_3, NO_2 and N_2O_4 without any reference value. For N_2, H_2 and O_2, calculated S_X are in good agreement with the experimental values, for all the methods we have tested. For N_2O_4 the energies are corrected for the internal rotation contribution as discussed in the previous subsection (see table 5).

We calculated $\Delta_f H^\circ_X$ at 0 K and at 298 K, S° at 298 K, and $\Delta_f G^\circ_X$ at 298 K for NH_3, NO_2 and N_2O_4. This data are presented in tables 7–9, along with experimental values available from thermochemical tables [20]. Relative deviations from the experimental values are given in parentheses. This relative deviation is calculated as $|X_{calc} - X_{exp}|/X_{exp}$, where X is the thermodynamic quantity such as $\Delta_f H^\circ_X$ or $\Delta_f G^\circ_X$. The accuracy of computed $\Delta_f G^\circ$ depends on the accuracy of the computed $\Delta_f H^\circ$ and S. Using a high-level method, such as W1 and CCSD(T), significantly improves the contribution of $\Delta_f H^\circ$. We observe this consistently in our data, shown in tables 7–9. $\Delta_f H^\circ_{298\ K}$ from W1 and CCSD(T) methods are always in better agreement with experimental values than the values computed from G3B3 and CBS-APNO, for all the three species. On the other hand, all the $S_{298\ K}$ estimates are quite close, and rather less sensitive to

[4] Standard enthalpies of formation of elements in their reference states are zero at all temperatures because they are the enthalpies of such *null* reactions as $N_2(g) \rightarrow N_2(g)$.

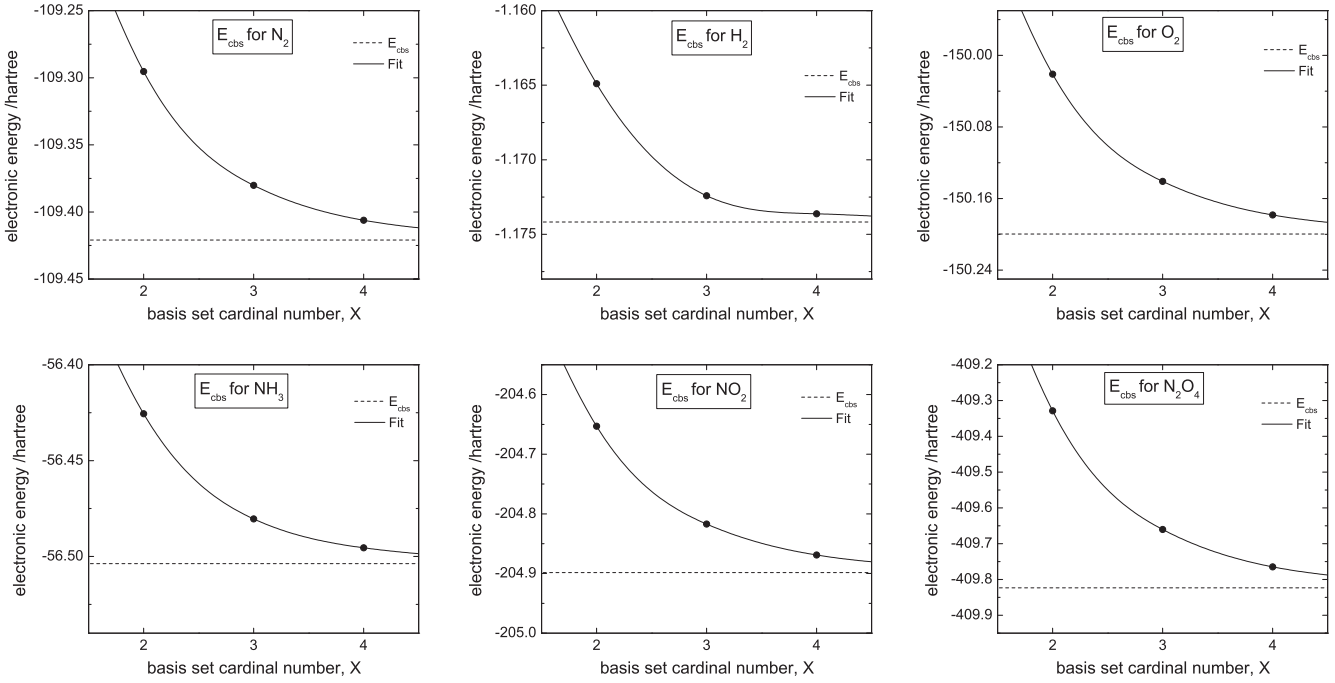

FIGURE 1. CBS-extrapolation of electronic energies using the mixed exponential plus Gaussian function (equation (9)) for H_2, N_2, O_2, NO_2, NH_3, and N_2O_4 calculated using the CCSD(T) method. The curves are fits of equation (9) to the data and the horizontal lines are the thus extrapolated asymptotic values.

TABLE 7
Enthalpy, $\Delta_f H^\circ$, absolute entropy, S, and Gibbs energy, $\Delta_f G^\circ$ of formation for NH_3 calculated using the G3B3, CBS-APNO, W1, and CCSD(T) methods. *Exp* refers to experimental values [22,20]. The relative deviations from experimental values are given in parentheses. Energies are in kJ · mol^{-1} and entropies in J · K^{-1} · mol^{-1}.

Method	G3B3	CBS-APNO	W1	CCSD(T)	Exp
$\Delta_f H^\circ_{0K}$/kJ · mol^{-1}	−34.30	−34.40	−40.76	−40.67	
$\Delta_f H^\circ_{298K}$/kJ · mol^{-1}	−41.65 (0.09)	−44.75 (0.03)	−48.10 (0.04)	−48.02 (0.04)	−45.90
S_{298K}/J · K^{-1} · mol^{-1}	192.42 (0.00)	191.99 (0.00)	192.32 (0.00)	192.55 (0.00)	192.77
$\Delta_f G^\circ_{298K}$/kJ · mol^{-1}	−12.21 (0.25)	−15.33 (0.06)	−18.66 (0.13)	−18.40 (0.12)	−16.40

TABLE 8
Enthalpy, $\Delta_f H^\circ$, absolute entropy, S, and Gibbs energy, $\Delta_f G^\circ$ of formation for NO_2 calculated using the G3B3, CBS-APNO, W1, and CCSD(T) methods. *Exp* refers to experimental values [22,20]. The relative deviations from experimental values are given in parentheses. Energies are in kJ · mol^{-1} and entropies in J · K^{-1} · mol^{-1}.

Method	G3B3	CBS-APNO	W1	CCSD(T)	Exp
$\Delta_f H^\circ_{0K}$/kJ · mol^{-1}	33.42	29.17	38.11	36.724	
$\Delta_f H^\circ_{298K}$/kJ · mol^{-1}	30.62 (0.08)	26.30 (0.20)	35.28 (0.06)	33.90 (0.02)	33.10
S_{298K}/J · K^{-1} · mol^{-1}	240.11 (0.00)	238.40 (0.00)	239.74 (0.00)	240.31 (0.00)	240.04
$\Delta_f G^\circ_{298K}$/kJ · mol^{-1}	48.68 (0.05)	44.52 (0.13)	53.41 (0.04)	52.01 (0.01)	51.31

TABLE 9
Enthalpy, $\Delta_f H^\circ$, absolute entropy, S, and Gibbs energy of formation, $\Delta_f G^\circ$ for N_2O_4 calculated using the G3B3, CBS-APNO, W1, and CCSD(T) methods. *Exp* refers to experimental values [22,20]. The relative deviation from experimental values are given in parentheses. Data corrected for the hindered rotor motion are indicated as *corr*. Energies are in kJ · mol^{-1} and entropies in J · K^{-1} · mol^{-1}.

Method	G3B3	CBS-APNO	W1	CCSD(T)	Exp
$\Delta_f H^\circ_{0K}$/kJ · mol^{-1}	11.73	13.80	21.12	17.72	
$\Delta_f H^\circ_{298K}$/kJ · mol^{-1}	2.38 (0.74)	2.95 (0.68)	11.59 (0.26)	8.40 (0.08)	9.16
$\Delta_f H^\circ_{298K}$ (corr)/kJ · mol^{-1}	2.45 (0.73)	3.14 (0.67)	11.67 (0.27)	8.47 (0.07)	9.16
S_{298K}/J · K^{-1} · mol^{-1}	301.34 (0.01)	291.62 (0.04)	301.74 (0.01)	303.88 (0.00)	304.29
S_{298K} (corr)/J · K^{-1} · mol^{-1}	301.76 (0.01)	292.75 (0.04)	302.23 (0.01)	304.35 (0.00)	304.29
$\Delta_f G^\circ_{298K}$/kJ · mol^{-1}	91.39 (0.07)	93.89 (0.04)	100.69 (0.02)	97.32 (0.00)	97.89
$\Delta_f G^\circ_{298K}$ (corr)/kJ · mol^{-1}	91.33 (0.07)	93.74 (0.04)	100.62 (0.02)	97.25 (0.00)	97.89

the choice of method because the respective standard scaling factors are applied to the calculated vibrational frequencies. For NH_3, the results from CCSD(T) and W1 are in good agreement with experimental values, as shown in table 7. $\Delta_f H^\circ_{298\ K}$ and $\Delta_f G^\circ_{298\ K}$ calculated using the W1 and CCSD(T) methods are within ±2 kJ · mol^{-1} of the experimental value. $S_{298\ K}$ predicted by CCSD(T) and W1 are quite

accurate. $S_{298\ K}$ calculated by G3B3 is closer to the experimental value as compared CBS-APNO, however, $\Delta_f G^\circ_{298\ K}$ estimate from CBS-APNO are better due to a more accurate calculation of $\Delta_f H^\circ_{298\ K}$.

For NO_2, the data from CCSD(T) show best agreement with experiments followed by W1. $S_{298\ K}$ for all four methods are consistently close with experiments. The differences in the respective $\Delta_f H^\circ_{298\ K}$ and $\Delta_f G^\circ_{298\ K}$ values for G3B3, CBS-APNO and W1 are significant. This is due to the better computation of electronic energy in the W1 scheme as compared to G3B3 and CBS-APNO. Apart from the diatomic O_2, NO_2 is the only molecule in our study where spin effects play a role, and the two latter methods are known to have issues with spin contamination [48,30]. In fact, G3B3 based on the density-functional approach using B3LYP correlation functional is known to have fewer spin-contamination issues for open-shell systems such as NO_2, as compared to CBS-APNO. Hence, the former $\Delta_f H^\circ_{298\ K}$ is closer to experiments. It has been reported by Mak and Wong [42] that the geometries predicted by the G3 and CBS-APNO methods are significantly different for the case of Nitrogen oxide species (both N–O and N–N bonds) due to the inadequacy of the QCISD geometry [30]. In fact, for the case of $ONOO^-$ ion, a difference of 71 kJ · mol^{-1} between the predicted heats of formation from G3 and CBS-APNO methods is reported [42]. We observe the maximum relative deviation from experiments for $\Delta_f H^\circ_{298\ K}$ and $\Delta_f G^\circ_{298\ K}$ for the CBS-APNO results. Our attempt to improve the QCISD/6-31 G step (of the CBS-APNO calculation) by geometry optimization at this level, as suggested in [42], followed by an appropriate calculation of the compound energies did not improve the description (geometry and energies) significantly.

For N_2O_4, $\Delta_f H^\circ_{298\ K}$ is largely underestimated by the G3B3 and CBS-APNO methods. W1 and CCSD(T) methods are far better and the calculated values are well within the range of expected errors. Our $\Delta_f H^\circ_{298\ K}$ is closer to the experimental value than the ones reported in reference [42]. In fact, G3B3 and CBS-APNO both predict similar numbers for $\Delta_f H^\circ_{298\ K}$ and $\Delta_f G^\circ_{298\ K}$. Again, the errors are not that significant for $S_{298\ K}$ as compared to those for $\Delta_f G^\circ_{298\ K}$. The better performance of W1 and CCSD(T) is again a result of a better description of the underlying geometry of the N_2O_4 molecule. As already stated in Section 2, the geometry optimization is done for both methods at the more sophisticated CCSD(T) level, while the other two methods rely on either B3LYP (G3B3) or RHF (CBS-APNO) geometries.

We also report the same quantities corrected for the hindered rotor motion. For $\Delta_f H^\circ$, the corrected values are close to the uncorrected ones for all methods. Relative errors for corrected data are similar to the uncorrected ones. The largest correction is $\simeq$0.19 kJ · mol^{-1} observed for the CBS-APNO data. Corrected $S_{298\ K}$ are closer to the experimental value, however, this improvement is not significantly reflected in the relative errors. The CCSD(T) result is almost identical to the experimental value. The correction for CBS-APNO is the largest $\simeq$1.13 J · K^{-1} · mol^{-1}. Finally the corrections are applied to $\Delta_f G^\circ$. Although the corrections for CBS-APNO were the largest amongst the four methods, the overall prediction of $\Delta_f G^\circ$ is not the worst. In fact, it is better than G3B3, due to the marginally better prediction of $\Delta_f H^\circ$. For the calculation of $\Delta_r G^\circ$ for the NO_2 dimerization reaction, corrected energies for N_2O_4 have been used. In fact, a particular choice of method (level of theory and basis sets) can give excellent results for some species, while not giving the best expected results for another species. This is attributed to the molecular symmetry of the species and the error compensation when its chemical structure is modeled using a specific compound thermochemistry method.

3.3. Equilibrium constants

For the NO_2 reaction, the experimental data for $\Delta_r G^\circ$ and K^{eq} show a spread, as seen in table 10. For 298.15 K, the measured value of K^{eq} varies between 0.136 and 0.147 [4] for the dissociation of N_2O_4. Reference [21] presents an IR spectroscopic study of the N_2O_4 dissociation reaction where K^{eq} at room temperature is measured within the same range as Ref. [4]. For the dimerization reaction we consider in our study, the corresponding K^{eq} is in the range between 6.54–7.36. From [24] and the corresponding $\Delta_r G^\circ$, K^{eq} is estimated to be in the range between 6.74–10.64. For the NH_3 reaction, a K^{eq} value of 5.4×10^5 is obtained from the $\Delta_r G^\circ$ value given in [20].

TABLE 10
Standard reaction Gibbs energies, $\Delta_r G^\circ$ (kJ · mol^{-1}) and equilibrium constant, K^{eq} for the NO_2 dimerization and NH_3 synthesis reactions. *Exp* refers to experimental values as well as data published elsewhere. $\Delta_r G^\circ$ calculated using experimental $\Delta_f G^\circ$ of the reaction species (taken from [20]) are the first among the several reported. For NO_2, the experimental values for $\Delta_r G^\circ$ are taken from [24] and references therein. Where different experimental values for $\Delta_r G^\circ$ have been published, the corresponding range of K^{eq} estimates are indicated as $x \pm \Delta x$, where x is the mean and Δx is the maximum variation. The range of experimental K^{eq} for NO_2 reaction includes data from Ref. [4]. Experimental data for NH_3 are from [20]

	Reaction			
	$2NO_2 \rightleftharpoons N_2O_4$		$N_2 + 3\ H_2 \rightleftharpoons 2NH_3$	
	$\Delta_r G^\circ$/kJ · mol^{-1}	K^{eq}	$\Delta_r G^\circ$/kJ · mol^{-1}	K^{eq}
Exp	−4.73, −5.86, −4.83, −5.79	8.69 ± 1.95	−32.90	5.69×10^5
G3B3	−6.03	11.39	−24.42	1.90×10^4
CBS-APNO	4.70	0.15	−30.66	2.36×10^5
W1	−6.20	12.19	−37.32	3.47×10^6
CCSD(T)	−6.77	15.35	−36.80	2.81×10^6

Table 10 shows $\Delta_r G^\circ$ and K^{eq} for the two chemical equilibrium reactions discussed in Section 2. As shown in equation (3), K^{eq} is exponentially related to $\Delta_r G^\circ$. A small error in the computation of $\Delta_f G^\circ_X$ for reaction species, and hence $\Delta_r G^\circ$, leads to a significant error in the calculation of K^{eq}. It is possible that $\Delta_r G^\circ$ is closer to the experimental value than $\Delta_f G^\circ_X$, due to cancellation of systematic errors in the calculation of individual $\Delta_f G^\circ$ or vice versa. We observe this in the case of the NO_2 reaction.

For the NO_2 reaction, the experimental data for $\Delta_r G^\circ$ and K^{eq} show a spread, as seen in table 10. Using the G3B3 method, we obtain $\Delta_r G^\circ = -6.03$ kJ · mol^{-1}, close to the experimental value from reference [24], and the $K^{eq} \simeq 11.39$ is also in good agreement with the range of experimental measurements. The CBS-APNO calculations yield $\Delta_r G^\circ = 4.70$ kJ · mol^{-1} and $K^{eq} = 0.15$ which are in poor agreement with the experiments. The CBS-APNO $\Delta_f G^\circ_X$ for NO_2 shows a large deviation from the experimental value, as shown in table 8, and this leads to the large deviation in the estimate for $\Delta_r G^\circ$. We also tested the CBS-QB3 method [49] and found similar results for $\Delta_r G^\circ$ and K^{eq}. $\Delta_r G^\circ$ from the W1 and CCSD(T) methods are −6.20 kJ · mol^{-1} and −6.77 kJ · mol^{-1} respectively, with relative deviations of $\simeq$ 6% and $\simeq$ 15% from the largest experimental value of $\Delta_r G^\circ$. The K^{eq} from W1 and CCSD(T), being 12.19 and 15.35 respectively, are higher than the experimental values but within the same order of magnitude. Our CCSD(T) $\Delta_r G^\circ$ value differs from [24] due to a difference in the fitting procedure used for getting the extrapolated complete basis set energies (see Section 2).

For the NH_3 reaction, we obtain $\Delta_r G^\circ = -24.42$ kJ · mol^{-1} and $K^{eq} \simeq 1.90 \times 10^4$ from the G3B3 method. This is about 30 times lower than the experimental value. Out of the other three methods, CBS-APNO performs best, underestimating the experimental $\Delta_r G^\circ$ by just 2 kJ · mol^{-1}, while both W1 and CCSD(T) overestimate $\Delta_r G^\circ$ by $\simeq$4 kJ · mol^{-1}. $\Delta_r G^\circ$ from W1 shows the largest relative deviation of $\simeq$ 13% from the experimental value. The K^{eq} for W1 is $\simeq 3.47 \times 10^6$, which is six times higher than the experimental value of 5.43×10^5 [20]. The CCSD(T) prediction of K^{eq},

2.81×10^6 is also five times higher. The CBS-APNO result of $\simeq 2.36 \times 10^5$ is closest to the experimental value.

3.4. Temperature dependence of $\Delta_f G_X$ and K^{eq}

In order to discuss the temperature dependence of $\Delta_f G$, we first discuss the temperature dependence of the enthalpy, H, given by Kirchoff's equation [50],

$$H^{\circ}_{T_1} = H^{\circ}_{T_0} + \int_{T0}^{T1} C_P(T)\,dT, \tag{10}$$

where C_P is the specific heat capacity, typically expanded in a polynomial series [51],

$$C_P(t) = a + bt + ct^2 + dt^3 + e/t^2, \tag{11}$$

where $t = T/(1000K)$, and the constants a, b, c, d, and e are listed in thermochemical tables [22]. Equations (10) and (11) motivate the relation

$$H^{\circ}_T = H^{\circ}_{298\ K} + at + bt^2/2 + ct^3/3 + dt^4/4 - e/t + f - h, \tag{12}$$

where f and h are additional constants also available from [22]. The temperature dependence of S is given as,

$$\Delta S = \int_{T0}^{T1} \frac{C_P(T)}{T}\,dT. \tag{13}$$

Equations (11) and (13) yield

$$S^{\circ}_T = a \ln t + bt + ct^2/2 + dt^3/3 - e/(2t^2) + g. \tag{14}$$

In the following, the temperature dependence of reaction thermodynamics is studied using the NH_3 synthesis reaction as an example. Using experimental $H^{\circ}_{298\ K}$ and appropriate constants ($a, b, \ldots g$) from [22] in equations (12) and (14), we calculate H°_T, S°_T and G°_T for NH_3, H_2 and N_2 at each T. Subsequently, we calculate $\Delta_r H$, $-T\Delta_r S$ and $\Delta_r G$ for the NH_3 formation reaction and denote them with the subscript *exp*.

Quantum chemical thermochemistry calculations use a simplified scheme (harmonic oscillator, ideal gas approximation, neglecting first and higher excited states) for including temperature dependent contributions. The electronic ground state energy is taken as the reference and contributions from the rotational, translational and vibrational degrees of freedom are added, including temperature dependence where applicable [38]. We use the W1 data from our calculation at 298.15 K to obtain $\Delta_r G^{\circ}$ at higher T by following the procedure prescribed in [38]. This fully *ab-initio* procedure that does not involve any experimental data requires the calculation of electronic energies, vibrational modes, moments of inertia, molecular mass, spin multiplicity, symmetry number and frequency scaling factor (if applicable, as for W1 data) as input from the thermochemistry calculation at 298 K for N_2, H_2 and NH_3. The T-dependent enthalpy (or entropy) is decomposed in two contributions: the T-independent electronic energy (at 0 K) and the T-dependent correction term. The calculated electronic reference energy at 0 K is the fundamental value, to which the respective thermal contributions are added to yield the T-dependent enthalpy and entropy. For a given T, the thermal contributions to internal energy, enthalpy and entropy are calculated using standard statistical mechanical formulae [38]. All the input parameters used in these formulae are obtained from the W1 calculation at 298 K, and no experimental data are used. This is repeated for the appropriate range of T, for each of the three species, N_2, H_2 and NH_3. Reaction energies are subsequently calculated at each T.

The enthalpic and entropic contributions are denoted as $\Delta_r H_{W1}$ and $-T\Delta_r S_{W1}$ respectively. $\Delta_r G$ calculated using the W1 theory at different temperatures are denoted as $\Delta_r G_{W1}$.

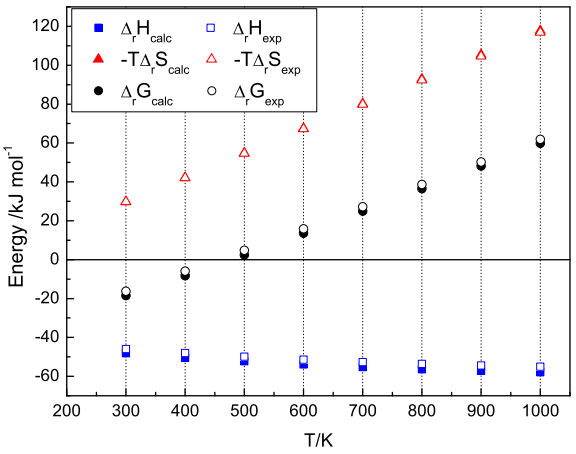

FIGURE 2. Dependence of the reaction enthalpy, $\Delta_r H$(■, □), entropic contribution to reaction Gibbs energy, $-T\Delta_r S$(▲, △) and reaction Gibbs energy, $\Delta_r G$(●, ○) on the temperature T for the NH_3 formation reaction. Subscripts *exp* and *calc* indicate experimental and W1 data, respectively.

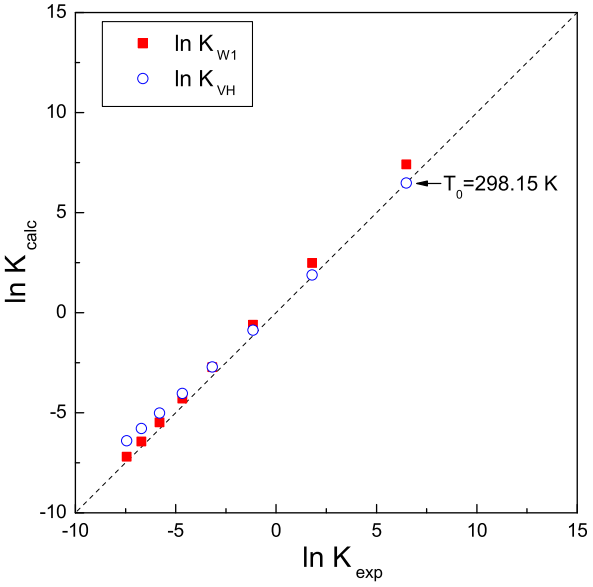

FIGURE 3. Comparison between the natural logarithm of calculated and experimental equilibrium constants for the synthesis of NH_3. W1 data are used to obtain $\ln K^{eq}_{W1}$(■) where as the Van't Hoff approximation according to equation (15) leads to $\ln K^{eq}_{VH}$ (○).

Fig. 2 shows a comparison between experimental and W1 calculated $\Delta_r H$, $-T\Delta_r S$ and $\Delta_r G$ for NH_3 as a function of temperature for $T \geqslant 298$ K. For all temperatures, the experimental and W1 data agree well. We observe that $-T\Delta_r S$ and $\Delta_r G$ have a strong T dependence. $\Delta_r H$ contains the temperature independent ground state electronic energy, and temperature dependent contributions from rotational, translational and vibrational degrees of freedom. Hence, $\Delta_f H$ is expected to show a weaker T dependence. At 298.15 K, the difference between the W1 and the experimental value for $\Delta_r G$ is $\simeq 2.3\ kJ \cdot mol^{-1}$, which is attributed to the $\Delta_r H$ contribution, and this difference remains approximately constant for higher T.

The $-T\Delta_r S$ values are almost identical for both data sets (with differences $\leqslant 1\ kJ \cdot mol^{-1}$). This can be explained as follows. For N_2, H_2 and NH_3, the W1 calculations for $S_{298\ K}$ are in excellent agreement to experimental values (see Section 3.2) due to the application of the appropriate scaling factor that compensates for

the method-dependent inaccuracies (Section 3.1 and table 3). Initial data have been used to obtain the T-dependence of S without any further loss of accuracy. Hence $-T\Delta_r S_{calc}$ values for the reaction do not differ significantly from the experimental values. When $\Delta_r G \geqslant 0$, the formation reaction of NH_3 will be endothermic, and this corresponds to $T \gtrsim 470$ K for the W1 calculation and $T \gtrsim 450$ K from the experimental data. For $T \simeq 298$—470 K where $\Delta_r G \leqslant 0$, NH_3 will be thermodynamically stable.

We use experimental and W1 calculated values of $\Delta_r G$ to compute K^{eq} from equation (3) and its natural logarithm is denoted as $\ln K^{eq}$. A widely used relation for the temperature dependence of K^{eq} is given by the Van't Hoff equation [50] which approximates the enthalpies to be temperature independent, leading to

$$\left(\frac{\partial \ln K^{eq}}{\partial T}\right)_P = \frac{\Delta H^\circ}{RT^2}. \tag{15}$$

$\ln K^{eq}_{VH}$ is calculated using the definite integral form of equation. (15) and experimental $\Delta H^\circ = -45.90\ \text{kJ}\cdot\text{mol}^{-1}$ at $T_0 = 298.15\ K$. Fig. 3 shows W1 calculated $\ln K^{eq}_{W1}$ and $\ln K^{eq}_{VH}$ versus $\ln K^{eq}_{exp}$ for 298 K $\leqslant T \leqslant$ 1000 K. As expected, at 298.15 K, only $\ln K^{eq}_{W1}$ shows a deviation from $\ln K^{eq}_{exp} = 6.48$ while $\ln K^{eq}_{VH}$ is exact. We observe that the deviation of $\ln K^{eq}_{VH}$ with respect to $\ln K^{eq}_{exp}$ increases for higher T as the approximation of a temperature-independent enthalpy is good for a limited range of temperature around 298.15 K only. On the other hand, the relative deviation of $\ln K^{eq}_{W1}$ from $\ln K^{eq}_{exp}$ remains almost constant up to ≃600 K, and decreases at $T \gtrsim$ 600 K. In order to compare the two schemes, one can plot $\ln K^{eq}$ versus $1/T$ and extract ΔH° from the linear fit of the curve. For the Van't-Hoff data, this analysis yields experimental $\Delta H^\circ = -45.86\ \text{kJ}\cdot\text{mol}^{-1}$ used as input. For $\ln K^{eq}_{W1}$, we obtain $\Delta H^\circ = -52.14\ \text{kJ}\cdot\text{mol}^{-1}$ with a standard error of 0.6. Hence, by using the W1 data for $\Delta_f G^\circ$ at 298.15 K for each specie, combined with appropriate temperature dependent contributions, we obtain $\Delta_r G$ in good agreement with experimental data over a range of T. Calculation of K^{eq} from the T dependent $\Delta_r G$ gives consistent results. The accuracy of the initial $\Delta_f G^\circ$ calculation at 298.15 K influences the accuracy of predicted K^{eq} as a function of T.

4. Conclusions

Using *ab-initio* calculations, we show that reliable values of $\Delta_f G^\circ_X$, $\Delta_r G^\circ$ and K^{eq} can be obtained for equilibrium reactions of NO_2 dimer formation and NH_3 synthesis. All methods we tested produce reliable structural parameters for all the reaction species involved. For $\Delta_f H^\circ$ and $\Delta_f G^\circ$, the quantum-chemical method CBS-APNO performs best for NH_3, while CCSD(T) data are closest to experiments for NO_2 and N_2O_4. For all molecules, $S_{298\ K}$ calculated using all the four methods are quite close to experimental values. Both G3B3 and CBS-APNO $\Delta_f H^\circ$ data show significant deviations from experiment for N_2O_4, a specie for which better basis sets and the calculation of electronic energies incorporating higher level of correlation are important factors.

There is a difference in the performance of these methods when comparing standard reaction Gibbs energies, $\Delta_r G^\circ$, and equilibrium constants, K^{eq}. For the NO_2 dimerization reaction, our best result is obtained from the G3B3 calculation, with $\Delta_r G^\circ = -6.03\ \text{kJ}\cdot\text{mol}^{-1}$ and $K^{eq} \simeq 11$. The values for $\Delta_r G^\circ$ from W1 and CCSD(T) are $-6.20\ \text{kJ}\cdot\text{mol}^{-1}$ and $-6.77\ \text{kJ}\cdot\text{mol}^{-1}$ respectively and the corresponding K^{eq} are ≃12 and 15. Our calculations support higher values of $\Delta_r G^\circ$ within the range of experimental data from different sources. All four calculated values for K^{eq} are of the same order of magnitude as the experimental data. The CBS-APNO calculations yield poor results, and are not well-suited for this reaction, due to issues with the molecular geometry (N–O and N–N bonds) of nitrogen oxides. For the NH_3 synthesis, we obtain $\Delta_r G^\circ = -30.66\ \text{kJ}\cdot\text{mol}^{-1}$ and $K^{eq} \simeq 2.36 \times 10^5$ from the CBS-APNO calculation. $\Delta_r G^\circ$ calculated from G3B3, W1, and CCSD(T) are −24.42, −37.32, and $-36.80\ \text{kJ}\cdot\text{mol}^{-1}$ respectively. The corresponding K^{eq} are about 1.9×10^4, 3.47×10^6, and 2.81×10^6. For this reaction, both W1 and CCSD(T) overestimate the energies and K^{eq}. G3B3 performs reasonably well in the calculation of $\Delta_r G^\circ$ for the NH_3 synthesis reaction, and predicts K^{eq} close to the experimental data. Interestingly, we see that CBS-APNO predicts the best result for this reaction.

We conclude that quantum-chemical methods such as G3B3 and CBS-APNO are quite robust in the calculation of equilibrium properties such as $\Delta_r G^\circ$ and K^{eq}, provided that the species of interest do not have known difficulties in modeling using a particular method. W1 and CCSD(T), which are relatively expensive calculations, are preferred for larger molecules where correlation, relativistic, and spin effects may be crucial for accuracy. Depending on the molecules involved, a reasonable choice can be made by referring to thermochemistry data for different methods. Systematic cancellation of errors and issues such as spin contamination, low lying virtual orbitals, and modeling of open-shell systems must be examined while selecting a compound thermochemistry method for the calculation of reaction energies.

We discuss the temperature dependence of $\Delta_r G^\circ$ and K^{eq} for the formation reaction of NH_3. Standard formation Gibbs energies, $\Delta_f G^\circ$, for higher temperatures are obtained by using W1 calculations of $\Delta_f G^\circ_{298\ K}$. We compare the experimental value of $\Delta_r G^\circ$ with explicit W1 calculated $\Delta_r G^\circ$ and find good agreement between the two. We show that the calculations of $\Delta_f G^\circ_{298\ K}$, and hence $\Delta_r G$ within reasonable accuracy, predict K^{eq} consistent with the experimental data over a range of temperatures. This is useful since calorimetric experimental data are usually available for limited temperature conditions only.

Equilibrium constants K^{eq} are measured at the restricted set of accessible laboratory conditions (temperature and solvents) and simulation data such as those presented here can provide access to a wider range of temperatures. For reactions where experimental measurements of equilibrium are carried out in the presence of solvents [52], formation Gibbs energy and equilibrium constant calculations are sensitive to the choice of the solvation model implemented in quantum chemical calculations [38].

References

[1] S. Tsintsarska, H. Huber, Molecular Physics 105 (2007) 25–31.
[2] P.R.P. Barreto, A.F.A. Vilela, R. Gargano, Intl. J. Quantum Chem. 103 (2005) 659–684.
[3] F.R. Ornellas, S.M. Resende, F.B.C. Machado, O. Roberto-Neto, J. Chem. Phys. 118 (2003) 4060–4065.
[4] H. Roscoe, A. Hind, J. Atmos. Chem. 16 (1993) 257–276.
[5] W.G. Burns, M. Matsuda, H.E. Sims, J. Chem. Soc. Faraday Trans. 86 (1990) 1443–1447.
[6] J.W. Sutherland, J.V. Michael, J. Chem. Phys. 88 (1988) 830–834.
[7] A.J. Vosper, J. Chem. Soc. A 625 (1970) 2191–2193.
[8] A. Guttman, S.S. Penner, J. Chem. Phys. 36 (1961) 98–99.
[9] V. Ermatchkov, A.P.-S. Kamps, G. Maurer, J. Chem. Thermodynamics 37 (2005) 187–199.
[10] V.N. Emel'yanenko, S.P. Verevkin, A. Heintz, J. Am. Chem. Soc. 129 (2007) 3930–3937.
[11] P.M. Nunes, F. Agapito, B.J. Costa Cabral, R.M. Borges dos Santos, J.A. Martinho Simões, J. Phys. Chem. A 110 (2006) 5130–5134.
[12] A. Pelekh, R.W. Carr, J. Phys. Chem. A 105 (2001) 4697–4701.
[13] G. da Silva, J.W. Bozzelli, N. Sebbar, H. Bockhorn, ChemPhysChem 7 (2006) 1119–1126.
[14] O.N. Ventura, M. Segovia, Chem. Phys. Lett. 403 (2005) 378–384.
[15] W.M.F. Fabian, Chem. Monthly 139 (2008) 309–318.
[16] B. Ruscic, J.E. Boggs, A. Burcat, A.G. Császár, J. Demaison, R. Janoschek, J.M.L. Martin, M.L. Morton, M.J. Rossi, J.F. Stanton, P.G. Szalay, P.R. Westmoreland, F. Zabel, T. Bérces, J. Phys. Ref. Data 34 (2005) 573–656.
[17] J. Demaison, L. Margulés, J.E. Boggs, Chemical Physics 260 (2000) 65–81.
[18] R. Janoschek, J. Kalcher, Z. Anorg. Allg. Chem. 628 (2002) 2724–2730.
[19] R.D. Johnson III (Ed.), NIST Computational Chemistry Comparison and Benchmark Database, NIST Standard Reference Database Number 101, release 15 b, The National Institute of Standards and Technology, USA, 2011.

[20] M. Chase Jr. (Ed.), NIST-JANAF Thermochemical Tables, Data Monograph No. 9, American Chemical Society, and American Institute of Physics, Woodbury, NY, 4 edition, 1998.
[21] R.J. Nordstrom, W.H. Chan, J. Phys. Chem. 80 (1976) 847–850.
[22] P.J. Linstrom, W.G. Mallard (Eds.), NIST Chemistry WebBook, NIST Standard Reference Database Number 69, The National Institute of Standards and Technology, USA, 2011.
[23] H. Lin, W. Thiel, S.N. Yurchenko, M. Carvajal, P. Jensen, J. Chem. Phys. 117 (2002) 11265–11276.
[24] E. Glendening, A. Halpern, J. Chem. Phys. 127 (2007) 164307–164317.
[25] P. Atkins, J. de Paula, Atkin's Physical Chemistry, Oxford Univ. Press., 7 edition, 2002.
[26] M.B. Ewing, T.H. Lilley, G.M. Olofsson, M.T. Rätzsch, G. Somsen, Pure & Appl. Chem. 66 (1994) 533–552.
[27] M.J. Frisch, G.W. Trucks, H.B. Schlegel, G.E. Scuseria, M.A. Robb, J.R. Cheeseman, J.A. Montgomery, Jr., T. Vreven, K.N. Kudin, J.C. Burant, J.M. Millam, S.S. Iyengar, J. Tomasi, V. Barone, B. Mennucci, M. Cossi, G. Scalmani, N. Rega, G.A. Petersson, H. Nakatsuji, M. Hada, M. Ehara, K. Toyota, R. Fukuda, J. Hasegawa, M. Ishida, T. Nakajima, Y. Honda, O. Kitao, H. Nakai, M. Klene, X. Li, J.E. Knox, H.P. Hratchian, J.B. Cross, V. Bakken, C. Adamo, J. Jaramillo, R. Gomperts, R.E. Stratmann, O. Yazyev, A.J. Austin, R. Cammi, C. Pomelli, J.W. Ochterski, P.Y. Ayala, K. Morokuma, G.A. Voth, P. Salvador, J.J. Dannenberg, V.G. Zakrzewski, S. Dapprich, A.D. Daniels, M.C. Strain, O. Farkas, D.K. Malick, A.D. Rabuck, K. Raghavachari, J.B. Foresman, J.V. Ortiz, Q. Cui, A.G. Baboul, S. Clifford, J. Cioslowski, B.B. Stefanov, G. Liu, A. Liashenko, P. Piskorz, I. Komaromi, R.L. Martin, D.J. Fox, T. Keith, M.A. Al-Laham, C.Y. Peng, A. Nanayakkara, M. Challacombe, P.M.W. Gill, B. Johnson, W. Chen, M.W. Wong, C. Gonzalez, J.A. Pople, Gaussian 03, Rev. E. 01, 2004.
[28] H.-J. Werner, P.J. Knowles, G. Knizia, F.R. Manby, Schütz, et al., MOLPRO v. 2010.1, a package of ab-initio programs, 2010.
[29] A. Baboul, L. Curtiss, P. Redfern, K. Raghavachari, J. Chem. Phys. 110 (1999) 7650–7657.
[30] J. Ochterski, G. Peterson, J. Montgomery, J. Chem. Phys. 104 (1996) 2598–2619.
[31] J. Martin, G. de Oliviera, J. Chem. Phys. 111 (1999) 1843–1856.
[32] C. Hampel, K. Peterson, H. Werner, Chem. Phys. Lett. 190 (1992) 1–12.
[33] Gaussian 03 User Manual, Gaussian Inc., Wallingford, CT, 2004.
[34] T. Dunning Jr., J. Chem. Phys. 90 (1989) 1007–1023.
[35] R. Kendall, T. Dunning Jr., R. Harrison, J. Chem. Phys. 96 (1992) 6796–6806.
[36] K.A. Peterson, D.E. Woon, T.H. Dunning Jr., J. Chem. Phys. 100 (1994) 7410–7415.
[37] J. Martin, J. Chem. Phys. 100 (1994) 8186.
[38] A. Marenich, C. Cramer, D. Truhlar, J. Chem. Theory. Comput. 4 (2008) 877–887.
[39] J.W. Ochterski, Gaussian Whitepapers and Technical Notes: Thermochemistry in Gaussian, 2000.
[40] B.W. McClelland, G. Gunderson, K. Hedberg, J. Chem. Phys. 56 (1972) 4541–4545.
[41] G. Herzberg, Electronic spectra and electronic structure of polyatomic molecules, Van Nostrand, New York, 1966.
[42] A.M. Mak, M.W. Wong, Chem. Phys. Lett. 403 (2005) 192–197.
[43] M. Jacob, Vibrational and Electronic Energy Levels of Polyatomic Transient Molecules, J. Phys. Chem.Ref. Data, Monograph 3, 1994.
[44] T. Shimanouchi, Tables of Molecular Vibrational Frequencies, Consolidated Volume 1, NSRDS NBS-39, 1972.
[45] L.M. Sverdlov, M.A. Kovner, E.P. Krainov, Vibrational Spectra of Polyatomic Molecules, Wiley, New York, 1974.
[46] P.Y. Ayala, H.G. Schelgel, J. Chem. Phys. 108 (1998) 2314–2325.
[47] K.S. Pitzer, W.D. Gwinn, J. Chem. Phys. 10 (1942) 428–439.
[48] P.M. Mayer, C.J. Parkinson, D.M. Smith, L. Radom, J. Chem. Phys. 108 (1998) 604–615.
[49] J.A. Montgomery Jr., M.J. Frisch, J.W. Ochterski, G.A. Petersson, J. Chem. Phys. 112 (2000) 6532–6542.
[50] E.B. Smith, Basic Chemical Thermodynamics, Fourth Ed., Oxford Univeristy Press Inc., New York, 1999.
[51] McQuarrie, Statistical Mechanics, Harper Collins Publishers Inc., New York, USA, 1976.
[52] T.F. Redmond, W.B. Bradford, J. Phys. Chem. 72 (1968) 1626–1629.

JCT 13-12